# Explosion-combustion in exoplanetary atmospheres

Grenfell, J. L.[1#], Godolt, M.[1*], Stracke, B.[1], Gebauer, S.[1], and Rauer, H.[1,2]

[1] Institut für Planetenforschung,
Deutsches Zentrum für Luft- und Raumfahrt (DLR), Rutherford Str. 2, 12489 Berlin, Germany

[2] Zentrum für Astronomie und Astrophysik (ZAA),
Technische Universität Berlin (TUB), Hardenbergstr. 36, 10623 Berlin, Germany

[#]Corresponding author, contact details:

Email: lee.grenfell@dlr.de

Tel: +49 30 67055 7934

FAX: +49 30 67055 384

[*]Now at (2)

***Abstract**: Conditions leading to explosion or/and combustion in exoplanetary atmospheres are investigated. For example, Super-Earths orbiting in the habitable zone of M-dwarf stars are proposed to have thick atmospheres consisting of abiotically-produced molecular oxygen together with molecular hydrogen accreted from the protoplanetary disk. In this paper we suggest that these atmospheres would undergo hydrogen-oxygen combustion triggered by e.g. lightning or cosmic rays which would limit the build-up of abiotic oxygen, lower the hydrogen gas envelope and could lead to liquid oceans with masses tens to hundreds of times larger than on the Earth. Combustion can produce hydrogen peroxide which can efficiently oxidize organic material and disfavor the development of life as we know it although the amount of $H_2O_2$ present relative to water is uncertain and depends on the balance between fast gas-phase sources and photolytic/depositional sinks. Explosion-combustion also generates hydrogen oxides which can efficiently oxidize methane and remove ozone catalytically. In addition to hydrogen-oxygen combustion in Super-Earth atmospheres, our results suggest that other explosive-combustive gas mixtures could lead to carbon monoxide or methane combustion in the atmospheres of some Mini Gas Planets, Titan-like worlds and in (Early) Earth-like atmospheres. Current atmospheric models do not directly consider these potentially important processes.*

**Key words**: Exoplanets, atmospheres, explosive-combustive reactions

## 1. Introduction and Motivation

Explosive-combustive reactions (e.g. Cohen, 1992) occur in gas mixtures over specific ranges of pressure (p) and temperature (T) if a fuel gas (such as molecular hydrogen, $H_2$) is present together with an oxidant gas (such as molecular oxygen, $O_2$) in suitable amounts. These reactions could be initiated in planetary atmospheres (with the appropriate p-T and composition) by lightning or cosmic rays and could have an important influence upon exoplanetary evolution yet their effects are usually not considered directly in atmospheric models.

In this work we investigate which atmospheres in exoplanetary science could feature explosion-combustion. The atmospheres of Super-Earths (SEs) are predicted in model studies (see section 4) to have large amounts of abiotically-produced oxygen ($O_2$) and molecular hydrogen ($H_2$) retained from the protoplanetary disk. Such a mixture could, according to our analysis, undergo explosion-combustion which on habitable worlds would condense to form large oceans containing the oxidant hydrogen peroxide ($H_2O_2$) (see 4.1 and appendix 1) which is unsuitable for life as we know it. For SEs in the Habitable Zone (HZ) of M-dwarf stars combustion-explosion could therefore represent an important mechanism for generating oceans. The amount of water delivery and migration of such worlds to the HZ is rather contested (Raymond et al., 2007, Ogihara and Ida, 2009). Also, gaseous mixtures containing ($CO$-$CH_4$-$O_2$-$N_2$) could explode or combust on Titan-like worlds and on some Mini Gas Planets (MGPs) (see section 4). On the Early Earth, combustion reactions limited surface atmospheric $O_2$ to less than 0.3 bar (see section 2).

Section 2 summarizes evidence for combustion of $O_2$(g) in Early Earth's atmosphere. Section 3 discusses the occurrence of lightning and cosmic rays which could initiate explosive-combustive reactions in (exo)planetary atmospheres. Section 4 briefly reviews explosive-combustive reaction mechanisms as a function of atmospheric composition, temperature and pressure and discusses them in the context of exoplanetary atmospheres. Sections 5 and 6 present the discussion and conclusions respectively.

## 2. $O_2$ combustion in Early Earth's atmosphere

Surface $O_2$ in Early Earth's atmosphere reached a maximum abundance of ~0.3 bar during the Carboniferous period about (300-400) Myr ago likely via increased organic burial associated with widespread vascular land plant coverage (Dahl et al., 2010). Higher $O_2$ abundances were prevented however, likely due to $O_2$ combustion of organic carbon to form $CO_2$ as suggested by studies of fossilized-charcoal from paleofires initiated by lightning (Heath et al., 1999; Berner, 1999).

## 3. Lightning and Cosmic Rays in Planetary Atmospheres

Explosion or/and combustion can be initiated when stable compounds such as molecular hydrogen are split to form reactive radicals which initiate radical chain reactions and release energy faster than it can be removed by the surroundings. An initial input of energy is required to split e.g. the hydrogen molecule which can be provided by e.g. lightning or cosmic rays.

### 3.1 Lightning

Modern Earth features on average ~44 lightning flashes $s^{-1}$ (intra-cloud and cloud-to-ground combined) with generally more activity over land and in the tropics (Christian et al., 2003; Oliver, 2005). Earth's lightning activity breaks molecular nitrogen into atomic nitrogen – this reacts with oxygen compounds to likely produce (2-10)Tg (N)/year of nitrogen oxides (NOx) which catalytically remove ozone in the stratosphere (e.g. Pickering et al., 1998). On Early Earth, lightning activity (Navarro-González et al., 1998) is estimated to be about ten times that of modern Earth and included a volcanically-induced component. On Venus, lightning activity is estimated to be about 20% that of modern Earth (Russell et al., 2008) although optical evidence is still rather lacking (Cardesín-Moinelo et al., 2016; Yair, 2012). On Mars, electrical discharge is thought to occur frequently in dust devils and synoptic to global-scale dust storms (Yair, 2012 and references therein). On Jupiter and Saturn, lightning activity is estimated to be about one hundred times that of modern Earth and peaks in the water cloud layers at 5 bar and 10 bar respectively (Yair, 2012 and references therein).

In summary, lightning is widespread in planetary atmospheres in the solar system. For SEs orbiting in the HZ of an M-dwarf star, General Circulation Model (GCM) studies (e.g. Joshi et al., 1997; Kite et al., 2011; Yang et al., 2013; Mills and Abbot, 2013) have suggested strong day-to-night circulation to maintain habitability which may provide wind velocities sufficient for charge separation hence favor the onset of lightning.

### 3.2 Cosmic Rays

Stellar (and Galactic) Cosmic Rays (CRs) penetrate deeply into Earth's atmosphere especially when solar activity is strong (e.g. Veronnen et al., 2008). For SEs orbiting in the HZ of an active M-dwarf star, high inputs of Stellar and Galactic CRs could be present due to e.g. strong stellar activity, the close proximity to the star and the potentially weakened planetary magnetosphere associated with tidal-locking (e.g. Grießmeier et al., 2005; Grenfell et al., 2007; Grenfell et al., 2012).

## 4. Explosive-Combustive Gas Mixtures

Rapid release of energy can occur in gas mixtures when runaway chemical production (chain propagation) of free radicals occurs faster than the corresponding sink (termination) reactions which remove the free radicals. Depending on p, T there are in general two main mechanisms for energy release, namely via explosion (detonation) in which a pressure wave moves supersonically away from the ignition site and combustion (deflagration) in which a sub-sonic pressure wave together with electromagnetic radiation are generated. Combustion can occur either via energy input via e.g. sparks created when an applied electric field leads to dielectric breakdown of the gas molecules. Alternatively, combustion can occur via lightning or/and cosmic rays which can also lead to splitting or/and ionization of e.g. air molecules, or can be spontaneous, referred to as 'self-combustion'. The energy required to induce explosion/combustion is termed the "minimum ignition energy" and is usually expressed in Joules.

Distinguishing between whether a given gas mixture explodes or combusts over a range of (p-T) is observationally challenging e.g. due to the power and complexity of the reaction mechanisms (see e.g. Sichel et al., 2002). Therefore in this work we use where possible the term "explosion-combustion" together. We now discuss explosion-combustion for different gas-mixtures and place them in the context of exoplanetary atmospheres.

### 4.1 $H_2$-$O_2$ Mixtures

Mixtures of $H_2$-$O_2$ gas, denoted as "oxyhydrogen", "electrolytic gas" or "detonating gas" are known to react either explosively or to combust, producing energy and e.g. the stable product water ($H_2O$). Assuming complete oxidation of $H_2$ by $O_2$, the overall (net) reaction is: $H_2+½O_2 \rightarrow H_2O$. However, in practice the mechanism consists of intermediate steps in which other stable reaction products such as $H_2O_2$ can form. The key reaction steps of the $H_2$-$O_2$ explosion-combustion mechanism (e.g. Cohen, 1992) are as follows:

$$H_2 \rightarrow H + H \quad (1)$$

$$H + O_2 \rightarrow OH + O \quad (2)$$

$$O + H_2 \rightarrow OH + H \quad (3)$$

$$OH + H_2 \rightarrow H + H_2O \quad (4)$$

$$H + H + M \rightarrow H_2 + M \quad (5)$$

158 $O^{\#} + O + M \rightarrow O_2 + M$ ` (6)

159 $H + OH + M \rightarrow H_2O + M$ (7)

160 $H + O_2 + M \rightarrow HO_2 + M$ (8)

161 $HO_2 + H_2 \rightarrow H_2O_2 + H$ (9)

162 $H/O/H/HO_2 + surface^{\#\#} \rightarrow products$ (10)

163

164 [$^{\#}$O-atoms supplied into the system via e.g. $CO_2$ photolysis; $^{\#\#}$ removed from the system via gas-surface heterogeneous
165 reactions occurring e.g. on the reaction chamber vessel or, in the case of a planetary atmosphere on the surface (if present) or
166 on atmospheric aerosol].

167

168 Reaction (1) is the initiation step in which $H_2$ is dissociated e.g. in planetary atmospheres by
169 lightning or by cosmic rays. $H_2$ has a minimum ignition energy in the range 0.02mJ/spark (US Dept. of
170 Energy, Hydrogen Fact Sheet 1.008) to 0.03 mJ/spark (Lackner, 2009). This compares with a value of
171 0.29mJ for $CH_4$, with values generally >0.2mJ for higher hydrocarbons (Ono and Oda, 2008) and with
172 values of typically ~1000mJ for dusts (many solids become very flammable when reduced to a fine
173 powder in air). In general these energies depend on the gas composition, the total pressure and the
174 spark duration (Maas and Warnatz, 1988; Ono and Oda, 2008). 'M' (reactions 5,6,7,9 above) refers to
175 any third body present in the gas-phase required to remove excess vibrational energy of the reactants.
176 Reaction rates of (1-10) are commonly implemented in photochemical models in the literature but often
177 lacking are (i) the chemical heats of reaction which drive the rapid and runaway energy release, or/and
178 (ii) treatment of lightning and/or cosmic rays which converts e.g. molecular into atomic hydrogen,
179 or/and (iii) the energy budget e.g. via thermal diffusion, conduction etc. (see next section). Reactions
180 (2)-(4) are the propagation steps. Reactions (2) and (3) are called "chain branching" since they produce
181 two reactive free radical products from one radical reactant and can therefore lead to runaway
182 propagation (production) of radicals. Reactions (5)-(7) represent the termination steps in which stable
183 (non-radical), gaseous products are formed from free radical reactants. Reaction (10) denotes sticky
184 collisions of gas species with solid surfaces (see appendix 2). Rapid release of energy occurs when the
185 runaway propagation steps start to rapidly exceed the termination steps. Note that the mechanism
186 produces $H_2O$ (reaction 7) and $H_2O_2$ (reaction 9) as stable products. Appendix 1 briefly presents some
187 key reaction rates for this mechanism.

188

189

190 **4.2 Modeling $H_2$-$O_2$ Explosion-Combustion**

191 Standard numerical packages are available to simulate explosion/combustion based on e.g. the
192 commercial CHEMKIN (CHEMical KINetics simulation software) numerical model (see e.g. Natarajan et
193 al., 2007). In such schemes, chemical networks containing reaction rate coefficients and exo-thermicity
194 (release of chemical energy) are typically coupled with transport modules which include e.g. conduction,
195 viscosity, thermal diffusion and effective potentials for intermolecular forces (see e.g. Paul and Warnatz,
196 1998).

197 Sichel et al. (2002) and Sichel et al. (2014) investigated $H_2$-$O_2$ explosions and found good
198 agreement between their numerical 1D model with heat-releasing reactions and observations derived
199 using a detonation tube. Seitzman (2005) applied e.g. CHEMKIN to investigate the onset of explosion of
200 $H_2$-air mixtures at 900K. Results suggested a rapid (with less than $10^{-4}$s induction time) build-up of H-
201 radicals from trace (background) amounts up to mass fractions of about 0.25 with similarly rapid
202 increases of temperature up to about 2500K. Burke et al., (2012) analyzed uncertainties in the rate
203 constants for $HO_2$ formation and loss and their effect upon our predictive capabilities of $H_2$-$O_2$ explosion.
204 Sichel et al., (2002) discussed "two-step kinetics" – here, in a first step free radicals are formed; in a
205 second step compression from the shock wave leads to strong heating hence to rapid increases in T
206 (typically by several hundreds of Kelvin) and p (typically by several tens of bar).

207 Key observables are firstly, the flame velocity i.e. the rate of expansion of a flame front in a
208 combustion reaction, and secondly the change in chemical concentrations with time. In general, the
209 numerical models simulate well (to within about 10%) such key observables for the $H_2$-$O_2$ reaction
210 mechanism which is relatively simple compared with other mechanisms. For example, the model of Paul
211 and Warnatz (1998) reproduced well observed flame velocities at 298K and 1bar of (1-10) $ms^{-1}$
212 (depending on the unburned fraction of $H_2$) in $H_2$-$O_2$ mixtures. Li et al. (2004) presented an updated
213 kinetic model for $H_2$-$O_2$ combustion and suggested that uncertainties in the flame speed could be
214 reproduced by adjusting the rate coefficient of the H+OH+M reaction within its uncertainty. Note that
215 the numerical models are frequently adapted to specific conditions (e.g. a particular reaction chamber,
216 shock tube etc.) rather than for planetary atmospheres in general.

217

218 **4.3 Relative concentrations of $H_2$:$O_2$ in Super-Earth atmospheres**

219 The amount of $H_2$ retained from the protoplanetrary disk depends sensitively on the planet's
220 mass, the size of the disk and the insolation from the star (Lammer et al., 2014; Luger et al., 2015) and

can cover a wide range - from complete loss of $H_2$ up to a few percent $H_2$ of the total planetary mass (Chiang and Laughlin, 2013).

The amount of (abiotic) $O_2$ in the SE atmosphere is also predicted to cover a wide range depending on the UV from the central star and on model treatments of photolysis and atmospheric escape. Abiotic $O_2$ production proceeds e.g. via either carbon dioxide ($CO_2$) photolysis followed by recombination of oxygen (O) atoms with each other (e.g. Canuto et al., 1982) or, via water $H_2O$ photolysis followed by escape of atomic hydrogen (H) (Berkner and Marshall, 1964). Selsis et al. (2002) modelled $CO_2$ (with varying humidity) and $H_2O$ atmospheres for planets orbiting Solar-like stars. Their results suggested modest to strong abiotic $O_2$ production with $O_2$ columns of up to $2.7x10^{24}$ molecules $cm^{-2}$, compared with $4.0x10^{24}$ molecules $cm^{-2}$ $O_2$ on the modern Earth (Schneising et al., 2008). Segura et al. (2007) however suggested abiotic $O_2$ amounts for $CO_2$-dominated atmospheres ten to eleven orders of magnitude smaller which they proposed arose because their model included rainout of oxidized species - this led to a high abundance of reducing species (like $H_2$) hence their $O_2$ abundances remained low. Model studies by Hu et al. (2012) and Tian et al. (2014) - who included redox balance and thermal escape - suggested modest abiotic $O_2$ amounts - about 100 times smaller than on modern Earth. Tian et al. (2014) suggested that the established OH-catalyzed cycles which drive the recombination of CO with O into $CO_2$ would be slow on SEs orbiting M-dwarf stars (i.e. favoring $O_2$ abiotic production up to 1000 times greater than for Sun-like stars) due to the weak Near-UV (NUV) output from the central star since NUV leads to release of atmospheric OH from its reservoirs (see also Harman et al., 2015). The model study by Domagal-Goldman et al. (2014) included redox balance of both the atmosphere and the ocean system and suggested low-to-modest abiotic $O_2$ amounts for an abiotic "Earth" orbiting in the HZ of an M-dwarf star, namely ~4-5 orders of magnitude lower than on modern Earth. They suggested that model differences with the above-mentioned Hu and Tian studies could have arisen due to different treatments of CO removal from the atmosphere. García Muñoz et al. (2009) investigated spectroscopic features of the $O_2$-$O_2$ dimer nightglow. Wordsworth and Pierrehumbert (2014) suggested that planets with low abundances of non-condensing gases such as molecular nitrogen ($N_2$) would feature weak cold traps hence rapid $H_2O$ photolysis which could lead to efficient abiotic $O_2$ production. Luger and Barnes (2015) modeled early stages of planets orbiting cooler stars and suggested very large abiotic $O_2$ several thousand times the mass of Earth's atmospheric $O_2$. In their study abiotic production is favored by strong incoming X-ray Ultra Violet (XUV) radiation from young (up to 1Gyr) pre-main sequence M-dwarf stars which drives fast photolysis of $H_2O$ and escape of the resulting H in the planetary atmosphere. Schwieterman et al. (2016)[a,b] discuss possible means of identifying abiotic $O_2$ spectral signals. More work

is required to constrain better the range of possible $CO_2$ and $H_2O$ amounts from outgassing (e.g. Lammer et al., 2013) available to form $O_2$ abiotically. Table 1 summarizes the range of $H_2$ and $O_2$ estimated from the literature to occur in SE atmospheres:

| Scenario | $H_2$ (g) | $\%O_{2lower}$ [$] | $\%O_{2upper}$ [$$] |
|---|---|---|---|
| 1. SE 0.0001% $H_2$ [*] | $2.01x10^{22}$ | 14.6 [**] | 99.2 |
| 2. SE 0.001% $H_2$ [*] | $2.01x10^{23}$ | 1.7 | 92.2 |
| 3. SE 0.01% $H_2$ [*] | $2.01x10^{24}$ | 0.2 | 54.2 |
| 4. SE 0.1% $H_2$ [*] | $2.01x10^{25}$ | 0.02 | 10.6 |
| 5. SE 1% $H_2$ [*] | $2.01x10^{26}$ | 0.002 | 1.2 |

Table 1: $H_2$ (total mass in atmosphere) and $O_2$ (% total atmospheric mass) for a SE assumed to have 1.5 times the planetary mass of the Earth and an SE atmosphere assumed to have the same mass as Earth's atmosphere. Earth's planetary mass=$5.97x10^{27}$g, Earth's atmospheric mass=$5.10x10^{21}$g (NASA Earth factsheet 2016). [$]Lower limit assumed here for abiotic $O_2$ = $3.44x10^{21}$g in the SE atmosphere based on Selsis et al. (2002) simulated for planets with $CO_2$ and $H_2O$ atmospheres orbiting Solar-like stars. [$$]Assumed upper limit for abiotic $O_2$ = $2.38x10^{24}$ based on Luger and Barnes (2015) simulated for planets with steam atmospheres orbiting pre-main sequence M-dwarf stars; the value shown corresponds to the abiotic $O_2$ production via XUV and EUV driven atmospheric escape of ten Earth oceans of hydrogen equivalent *Mass of the $H_2$ atmosphere as a percentage of the total mass of the planet. [**]As an example of the calculation in Table 1: $\%O_{2lower}$ (scenario 1) = 100-(($2.01x10^{22}$/($2.01x10^{22}$+$3.44x10^{21}$)*100) = 14.6%.

The $H_2$ range in the literature extends from complete loss of $H_2$ up to a few percent of the total SE planetary mass as discussed above. Scenarios 1-5 in Table 1 therefore shows a representative range - from an upper value of 1% $H_2$(g) of the planet's mass (scenario 5) decreasing by four orders of magnitude (scenarios 4 to 1). The lower and upper scenarios for $O_2$ show a representative range found in the literature for model studies simulating planets orbiting in the HZ of main sequence stars. Which ($H_2$-$O_2$) compositions in Table 1 will lead to combustion-explosion? At Standard Temperature and Pressure (STP) conditions, mixtures with between ~5-20% $O_2$ (g) by volume will combust-explode. At higher (T,p) however the upper limit can reach values higher than 20% (to illustrate this point, refer to e.g. Figure 1, which is determined for a stoichiometric 2:1 $H_2$:$O_2$ molar mixture i.e. with ~33% $O_2$ by volume). The lower value (~5%) represents the limiting oxygen composition (Moeller et al., 1998). Above the upper value the mixture is too oxygen-rich for initiation reactions of combustion-explosion. Values in

Table 1 suggest that scenarios 1 ($O_{2lower}$) and scenario 4 ($O_{2upper}$) i.e. with 14.6% and 10.6% $O_2$ respectively both lie in this 5-20% $O_2$ range, where combustion-explosion is possible at STP (see also discussion to Figure 2 below). Scenarios 1-3 ($O_{2upper}$) are too oxygen-rich to combust-explode. However, in reality we expect that the abiotic $O_2$ value would build up from zero and would combust-explode once the lower limit of ~5% $O_2$ is reached.

**4.4 Temperature-pressure dependence of $H_2$-$O_2$ explosion**

Figure 1 shows the T-p dependence of the $H_2$-$O_2$ explosion limits assuming a 50:50 molar (check!) $H_2$-$O_2$ mixture:

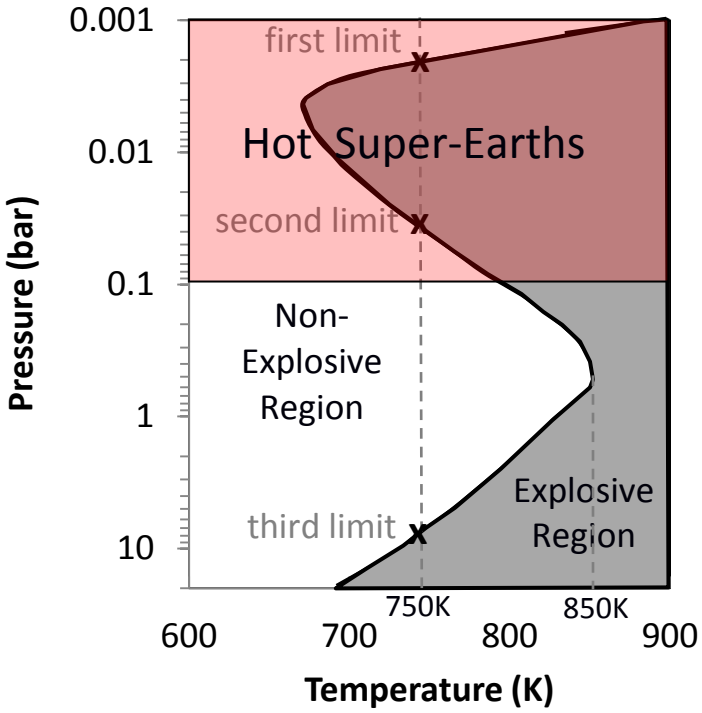


Figure 1: Temperature-pressure dependence of ($H_2$-$O_2$) explosion. Data source adapted from Lewis and von Elbe (1987) for a two-to-one hydrogen-to-oxygen stoichiometric mixture using a spherical vessel 7.4cm in diameter with a potassium chloride coating. The explosive region is shaded in grey, the non-explosive region is non-shaded. As an example at T=750K, the three points marked as "X" along the grey dashed line denote the first, second and third explosive limits i.e. where the grey-shaded and non-shaded regions cross.

**Hot SEs** - the red shaded area in Figure 1 shows the relevant region for observing hot Super-Earths. The pressure region covered here (0.1-0.001bar) corresponds to the expected range for observations via transit transmission spectroscopy (Hu and Seager, 2014). SE atmospheres are predicted to cover a wide range of p and T, from potentially habitable conditions such as recently suggested for Kepler 452b (Jenkins et al., 2015) to the hot, thin atmospheres of SEs such as CoRoT 7b (Hatzes et al.,2011) where surface T at the sub-stellar point likely exceeds 2000K. Table 1 has shown that the 50:50 composition for $H_2$:$O_2$ which is assumed in Figure 1, is within the predicted composition range for SE model scenarios. The white (non-explosive) and grey (explosive) regions in Figure 1 can be interpreted as follows:

**Pressure Effect** - At pressures lower than the first limit in Figure 1, the mixture is non-explosive (corresponding to the unshaded region at the top of Figure 1) due to efficient diffusion favoring wall-reactions on the reaction vessel (for an estimation of this effect for atmospheres, see appendix 2) which remove reactive radicals. On increasing pressure, diffusion slows and the mixture becomes explosive i.e. the rate of the propagation reactions exceed that of the termination reactions - at the 'first (explosive) limit'. On increasing pressure further, the mixture becomes once more non-explosive at the 'second limit' because the pressure-dependent reaction 9 (whose rate varies approximately with $p^2$) is now important in removing H atoms; Lee and Hochgreb (1998) discuss effects affecting the second explosion limit and present possible chemical pathways for $H_2$ oxidation. At higher pressures still, reaction 8 could become important in producing H and the mixture becomes once more explosive at the 'third limit'. Schroeder and Holtappels (2005) present the lower and upper explosion limits shown in the number of moles of $H_2$ present as a % of the total moles (mol% $H_2$) as a function of pressure. The lower limits vary from 4.3% mol%$H_2$ (1 bar) up to 5.6% mol%$H_2$ (150bar); the upper limits vary from 76.5% mol%$H_2$ (1 bar) down to 72.9% mol%$H_2$ (150bar). Zheng et al. (2010) suggested that experimental design (chamber size, shape, wall-coating etc.) leads to an error in the derived e.g. (p-T) of both the lower and upper explosion limits by about 4%.

**Temperature Effect** - At temperatures above about 850K (see Figure 1) the system is explosive for all pressures. This is because propagation reactions have generally moderately positive temperature-dependencies whereas termination reactions have either only weakly positive or weakly negative temperature dependencies. At intermediate temperatures (700-850K) the system can be explosive or not depending on the pressure. Maas and Warnatz (1998) provide more details on the T-dependence of propagation and termination reactions. Schroeder and Holtappels (2005) present the lower and upper

explosion limits (in mol%$H_2$) as a function of temperature. The lower limits vary from 3.9% (293K) down to 1.5% (673K); the upper limits vary from 75.2% (293K) up to 87.6% (673K).

**4.5 Composition dependence of ($H_2$-$O_2$) combustion**

Figure 2 shows the combustion (flammability) limits of ($H_2$-$N_2$-$O_2$) mixtures at T=298K and p=1 bar:

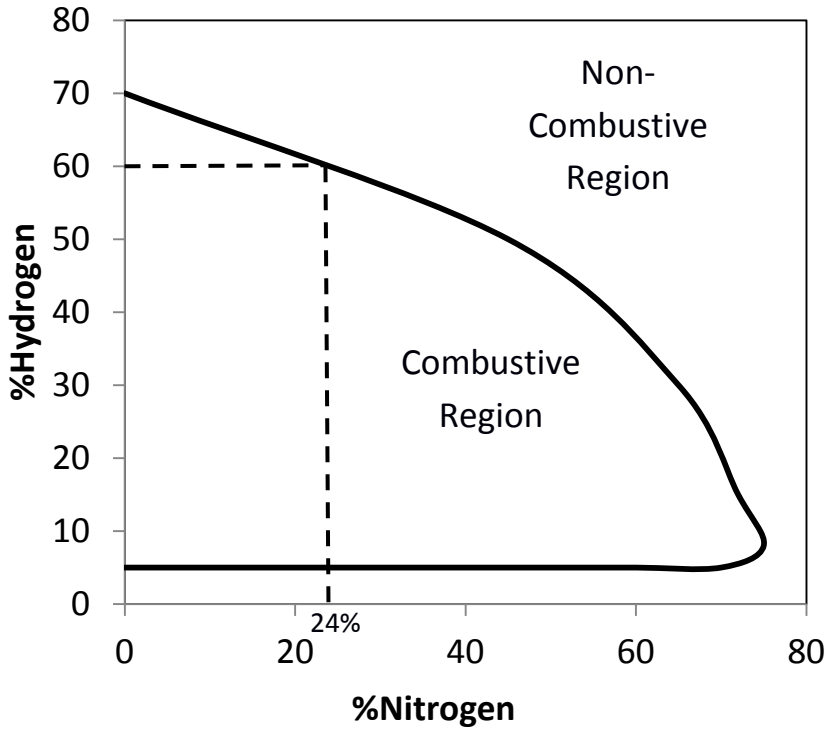


Figure 2: Compositional dependence of the ($H_2$-$N_2$-$O_2$) system (shown in molar concentration by percent) upon combustion for gas mixtures at T=298K, p=1bar. The Figure shows %$H_2$ concentration (y-axis) and %$N_2$ concentration (x-axis) with the remaining ("rest gas") being $O_2$. For example, for the dotted line shown the %molar gas composition is [60:24:16] for [$H_2$:$N_2$:$O_2$]. Data source is as for Figure 1.

Figure 2 suggests that ($H_2$-$O_2$-$N_2$) mixtures at T=298K and p=1bar are combustive (flammable) for $O_2$ concentrations with (lower to upper) combustion limits of about (5-30%) and for $H_2$ concentrations of about (5-70%). Other studies (Schroeder and Holtappels, 2005) reported similar limits at these (p,T) i.e. suggesting a lower limit of (3.6-4.2%) $H_2$ and an upper limit of (75.1-77.0%) $H_2$ depending on the experimental set-up. Above about 70% $N_2$, the mixture in Figure 2 is non-combustive, whereas for high $H_2$ concentrations this value decreases to ~0% $N_2$. On increasing the temperature for ($H_2$-$O_2$-$N_2$)

mixtures (e.g. to 300$^{o}$C, not shown) the % lower (upper) combustive limit for $H_2$ concentration in Figure 2 is lowered (raised) by a few percent.

**4.6 Timescales for Explosion-Combustion in $H_2$-$O_2$ atmospheres**

Consider a SE which retained its initial thick $H_2$ envelope and where abiotic $O_2$ is building up in the atmosphere via photochemical processes e.g. initiated by $CO_2$ or/and $H_2O$ photolysis. If the build-up of $O_2$ is slow compared with processes which initiate explosion-combustion (such as lightning, cosmic rays etc.), then if $H_2$-$O_2$ abundances rise above the lower limit where explosive-combustive begins, they will be quickly burnt-off. The composition of the atmosphere will then remain approximately constant at this lower limit. If however the processes which initiate explosion-combustion are seldom then the composition of the atmosphere could build-up via photochemistry to above the lower limit without explosion-combustion taking place. Table 2 shows typical atmospheric timescales of the relevant atmospheric processes:

| Process | Scenario | Timescale |
|---|---|---|
| $CO_2$ photolysis | Modern Earth | 109 years$^{*}$ |
| Lightning | Modern Earth | (1/44) seconds$^{**}$ |
| Cosmic Rays | Modern Earth | 0.7 years$^{\#}$ |
| Cosmic Rays | AD Leonis | 0.7 hours$^{\#\#}$ |

Table 2: Timescales of processes related to photochemistry ($CO_2$ loss via photolysis) and explosion-combustion. $^{*}$Characteristic photolytic destruction time (=[$CO_2$ ]/j$CO_2$) where square brackets denote abundance and j$CO_2$ denotes the photolysis rate at 60km based on the Earth control run from Grenfell et al. (2014). j$CO_2$ is proposed to represent a first step in abiotic production of combustible $O_2$ in Earth-like atmospheres (see below). $^{**}$Average time between lightning flashes based on Earth observations of (44±5) lightning flashes per second globally (Oliver, 2005). $^{\#}$Average time between Ground Level Events (GLEs) in which cosmic ray increases are recorded at the Earth's surface. Data is for Solar Cycle 23 over which 16 GLEs were observed over 11 years i.e. one GLE every 0.7 years on average (Gopalswamy et al., 2010). $^{\#\#}$Time between Coronal Mass Ejections (CMEs) based on estimations for the active M-dwarf star AD Leonis which features 36 CMEs per Earth day (Khodachenko et al., 2007).

Table 2 suggests that the time elapsing between lightning and cosmic rays which could initiate explosion-combustion is short compared with the $CO_2$ photolysis timescale which is a proxy for build-up of abiotic $O_2$. Clearly, this build-up can be more complex since not all atomic oxygen produced from $CO_2$ photolysis will lead to gas-phase $O_2$ production. Also, $O_2$ can be removed e.g. on the surface or via photolysis. However, we assume here that all atomic oxygen (O) produced from $CO_2$ photolysis leads to abiotic $O_2$ production as a conservative estimate since the actual timescale (i.e. for which not all O contributes to forming $O_2$) is expected to be even longer, so our conclusions will not change. Table 2 therefore suggests that once a combustive-explosive mixture is attained e.g. via photochemistry for the case shown, combustion-explosion would proceed almost instantly, burning-off any excess gases above the lower combustion-explosion limit and holding the atmospheric composition at this lower limit.

In general, combustion-explosion is a very rapid processes (of the order of milliseconds) and could be initiated by lightning and cosmic rays frequently in the atmosphere. Photochemical timescales of the relevant chemical species (like $H_2$, $O_2$ and $CH_4$) however, are usually rather long and they are expected to be well-mixed. This suggests that the timescales of explosion-combustion will generally be rapid enough to limit the build-up of combustive species.

### 4.7 CO-$O_2$ Mixtures

CO combustion in $O_2$ has been proposed (e.g. Cohen, 1992) although the mechanism is not as well understood as for $H_2$-$O_2$ mixtures. CO combusts in air for abundances between about (16-70%) at room temperature and between about (12-74%) at 300$^o$C (Cohen, 1992, their Figure 10 and references therein). In damp atmospheres, it is likely that HOx resulting from $H_2O$ photolysis would catalyze CO into $CO_2$ so the CO is less likely to build up to its combustive limit.

#### 4.7.1 Explosive-combustive CO-$O_2$ reactions in Mini Gas Planets (MGPs)

The model study of Hu and Seager (2014) (their Figures 5 and 6) varied e.g. C/O ratios and predicted atmospheric compositions which suggested MGPs could form with atmospheric concentrations of several tens of percent by volume of CO and $O_2$. Their results were averaged from p=(1000-100)mb and T from about (700-800)K. Our work suggests that these atmospheres would combust. For example, in their Figure 5, for a GJ1214b-like planet, the combustion limit for CO-$O_2$ is reached – with CO and $O_2$ vmrs both reaching up to 20% - for C/O values ranging from (0.3-0.5) and for $X_H$ ranging from (0.2-0.5) (see the panels in their Figure 5 marked CO and $O_2$). In their Figure 6 for a 55

Cnc e-like planet the combustion limit for $CO\text{-}O_2$ is similarly reached – again with CO and $O_2$ vmrs of up to 20% -for C/O values ranging from (0.2-0.6) and for $X_H$ ranging from (0.0-0.6).

### 4.8 Hydrocarbon-$O_2$-$N_2$ Mixtures

The lower and upper limits of combustion for different gases, namely $H_2$, CO, $CH_4$, ethylene ($C_2H_4$) and propane ($C_3H_8$) with air as a fill gas were determined by Zlochower and Green (2009) (see their Table 1). Their results are summarized below in Figure 3:

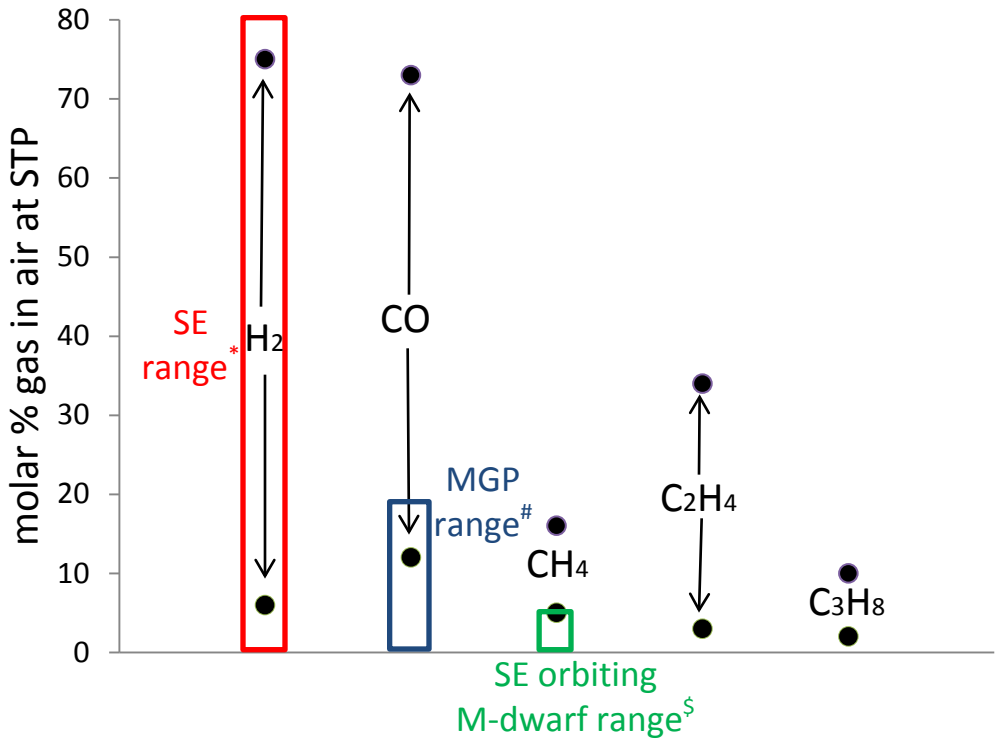


Figure 3: Combustion range shown by the black arrows for the molar concentration of five gases determined in air at STP by Zlochower and Green (2009). Red, blue and green rectangles show the range of possible atmosphere compositions for SEs, MGPs and SEs orbiting in the HZ of M-dwarf stars respectively. *See Figure 1 and accompanying text. #See section 4.8.1. $See section 4.9.3.

At higher temperatures than in Figure 3 the lower limits are lowered, typically by a few percent per 100K. Di Benedetto et al. (2011) investigated explosions of $CH_4$ in $O_2$-enriched air from 293-423K and with 10-33% $CH_4$ in a laboratory chamber. Results suggested complete oxidation of $CH_4$ and $O_2$ into $CO_2$

and $H_2O$ with oscillating pressure waves being formed attributed to the occurrence of condensation and vaporization cycles of the $H_2O$ formed.

**4.8.1 Explosive-combustive Hydrocarbon-$O_2$-$N_2$ mixtures in Titan-like atmospheres**

Modern Titan has a near-surface $CH_4$ concentration of about 5% (Tobie et al., 2006). Interestingly, this value is comparable to the laboratory-determined limit above which $CH_4$ combustion would start. Numerous studies of $CH_4$-$O_2$ combustion have initial temperatures at or close to room temperature (e.g. Rozenchan et al., 2002; Pfahl et al., 2000). For the cold surface temperature of modern Titan of about 70K however, combustion data is lacking. In summary, a warm (habitable) Titan-like world with sufficient molar concentrations of $O_2$ (i.e. more than a few %) in the atmosphere together with lightning or cosmic rays, could feature $CH_4$ combustion for atmospheric $CH_4$ abundances of more than about 5% by molar concentration, although further data is required to test this. An important caveat is whether the established photochemical oxidation of $CH_4$ (e.g. via the hydroxyl radical on Earth which is a function of e.g. UV, $H_2O$ etc.) would prevent such levels of $CH_4$ and $O_2$ being reached before combustion could take place.

**4.8.2 Explosive-combustive Hydrocarbon-$O_2$-$N_2$ mixtures in Hot Jupiter (HJ) atmospheres**

Jupiter presently features $CH_4$ concentrations at least two orders of magnitude lower than its combustion lower limit (Yung and DeMore, 1999). $CH_4$ concentrations in the atmospheres of HJs are estimated to be somewhat higher than on Jupiter i.e. up to a few tenths of a percent and could be even higher still for HJs with high (C/O) ratios (see e.g. Moses et al., 2013, who suggest $CH_4$ abundances of up to several tenths of a percent for C/O>1.9, their Figure 2). This, together with the high temperatures on HJs suggests that the lower limit for $CH_4$ combustion could be approached in the high C/O cases mentioned above. Still required of course would be $O_2$ concentrations above a few % by molar concentration. Such values are predicted for some MGP formation scenarios e.g. by Hu and Seager (2014), their Figure 6). For most HJ model studies of chemical composition (e.g. Moses et al., 2013) the $O_2$ values are usually not discussed but are expected to have very low abundances especially at higher p.

**4.8.3 Explosive-combustive Hydrocarbon-$O_2$-$N_2$ reactions in SE atmospheres in the HZ of M-dwarfs**

Several studies (e.g. Segura et al., 2005; Grenfell et al., 2014) have suggested abundant atmospheric $CH_4$ molar concentrations of up to ~1% for these objects. The highest $CH_4$ concentrations are found especially for planets which orbit the cooler M-dwarf stars, as discussed in those works. The

458 significant amounts of atmospheric $CH_4$, together with greenhouse heating (which would favor
459 combustion by lowering the minimum combustion abundance of $CH_4$) therefore suggests that possible
460 $CH_4$ combustion on such worlds (see Figure 3) could be possible for SEs orbiting cooler M-dwarf stars if
461 these worlds have $CH_4$ emissions similar to the Earth or stronger.
462
463 **4.8.4 Explosive-combustive Hydrocarbon-$O_2$-$N_2$ reactions in the Early Earth's atmosphere**
464 Elevated atmospheric $CH_4$ molar concentrations of up to a few tenths of a percent on the Early
465 Earth are suggested by modeling studies (e.g. Pavlov et al., 2000). Note however that organic aerosol
466 could form at higher $CH_4$ concentrations (Zerkle et al., 2012) which could prevent atmospheric $CH_4$ from
467 building up further. Model studies therefore suggest that atmospheric $CH_4$ on Early Earth probably did
468 not reach the combustive limit.
469
470 **4.9 $H_2$-$CH_4$-$NH_3$-$N_2O$-$O_2$-$N_2$ Mixtures**
471 We briefly note here that atmospheric species which are found on Earth and on gas giants - such
472 as ammonia ($NH_3$) as well as the Earth biosignature nitrous oxide ($N_2O$) – could both undergo
473 combustion reactions in mixtures of $H_2$-$CH_4$-$NH_3$-$N_2O$-$O_2$-$N_2$ (Pfahl et al., 2000) although the details of
474 the chemical and physical mechanism are not well known. The molar concentrations required for
475 combustion (at least a few %) for these two species are however likely not reached in most currently-
476 conceivable exoplanetary atmospheric scenarios since e.g. $NH_3$ sources are weak and since this molecule
477 is removed via e.g. photolysis and rainout quite quickly (typically on the order of hours to days on
478 modern Earth). Also for $N_2O$ the atmospheric sources hence the molar concentrations are usually rather
479 low (e.g. ~$3x10^{-7}$ on modern Earth).
480
481 **5. Discussion**
482 We have reviewed atmospheres in which the build-up on the one hand of combustible chemical
483 products (e.g. via the build-up of abiotic $O_2$ via $CO_2$ and/or $H_2O$ photolysis) could be limited on the other
484 hand by combustion-explosion (e.g. triggered by lightning and cosmic rays). The planetary climate will
485 determine whether the $H_2O$(g) produced from ($H_2$-$O_2$) explosion-combustion stays in the gaseous form
486 or rains out of the atmosphere. If it stays in its gaseous form, then it will contribute to climate warming
487 and could dissociate into HOx which can destroy ozone ($O_3$(g)). The amount of $H_2O$(g) and $H_2O_2$(g)
488 produced depends on the rates of the individual reaction steps which is discussed further in appendix 1.
489 Planetary formation (see e.g. Chiang and Laughlin, 2013) and photochemical models suggest that the

protoatmosphere could form with enough $H_2$ accreted and abiotic $O_2$ which could combust to form several tens of Earth's ocean mass (one Earth ocean has 270 bar). This could represent an important mechanism to form oceans on such planets since some studies (e.g. Luger and Barnes, 2015) have suggested extreme water loss due to strong stellar activity in the early stages after accretion. There could be a competition between established photochemistry (i.e. calculated in photochemical models which do not have chemical heating) and (faster) explosion-combustion. The impact of this upon planetary evolution requires further investigation.

## 6. Conclusions

- Explosion-combustion are potentially important processes in exoplanetary atmospheres over a wide range of conditions and need to be considered in current atmospheric models of exoplanetary science.
- Although most current chemical networks include the relevant reactions e.g. for the $H_2$-$O_2$ system, these models do not simulate explosion-combustion because they (either) do not couple chemical heats of reaction with the atmospheric climate or/and do not consider the energy budget (e.g. conduction away from the source) of an explosive-combustive mixture. As a first step, such models could however impose limits in composition based on explosion-combustion theory.
- Build-up of abiotic $O_2$ is limited for SEs by explosion-combustion if accreted $H_2$ atmospheres are present. This could lead to formation of large (several Earth masses) oceans, which could be alkaline due to $H_2O_2$ production. This has consequences both for theoretical estimates of atmospheric biosignatures and for our understanding of the potential development of life on such worlds.
- ($CO$-$O_2$) explosive-combustive reactions could have played a role in the evolution of some MGPs.
- (Hydrocarbon-$N_2$-$O_2$) explosive-combustive reactions could have played a role in the evolution of Titan-like worlds and Earth-like worlds orbiting in the HZ of especially cooler M-dwarf stars.

## References

Di Benedetto, A., et al., Combustion and Flame, 158, 2214-2219, 2011.

Berkner, L. V., and Marshall, L., Discuss. Faraday Soc., 37, 122, 1964.

Berner, R. A., PNAS, 96, 20 1999.

Burke, M. P., et al., Int. J. Chem. Kin., 44, 444-475, 2012/

521 Canuto, V. M., et al., Nature, 296, 816, 1982.
522 Cardesín-Moinelo, A., et al., Icarus, 277, 395-400, 2016.
523 Chian, E., and G. Laughlin, MNRAS, 431, 3444, 2013.
524 Christian, H. J., et al., J. Geophys. Res., 2003.
525 Cohen, N., Aer. Rep., TR-92 (2534-1), 1992.
526 Dahl, T. W., et al., PNAS, 107, 17,911-17,915, 2010.
527 Domagal-Goldman, S., et al., ApJ, 792, 90, 2014.
528 Esposito, F., et al., Int. J. Mars Sci. Exploration, 6, 1-12, 2011.
529 Garcia-Munoz, A., et al., J. Geophys. Res., 114, E12002, 10.1029/2009JE003447, 2009.
530 Gopalswamy, N., Ind. J. Radio Space Phys., 240-248, 2010.
531 Grenfell, J. L., et al., Astrobiol., 7, 208-221, 2007.
532 Grenfell, J. L., et al., Astrobiol., 12, 1109-1122, 2012.
533 Grenfell, J. L., et al., Plan. Spa. Sci., 98, 66-76, 2014.
534 Grieβmeier, J.-M., et al., Astrobiol., 5, 587-603, 2005.
535 Harman, C. E., et al., ApJ, 812, 137, 2015.
536 Heath, M. J., et al., Origins Life, 29, 405-424, 1999.
537 Hu, R., et al., ApJ, 761, 166, 2012.
538 Hu, R., and Seager, S., ApJ, 763, 25, 2014.
539 Jenkins, J. M., et al., A&A, 150, 56, 2015.
540 Joshi, M., et al., Icarus, 129, 450, 1997.
541 Khodachenko, M., et al., Astrobiol., 7, 167-184, 2007.
542 Kite, E., et al., ApJ, 743, 1, 2011.
543 Lackner; M., „Alternative ignition systems“, ProcessEng Engineering GmbH, 978-3-902655-05-9, 2009.
544 Lammer, H. et al., MNRAS, 430, 1247-1256, 2013.
545 Lammer, H. et al., MNRAS, 439, 3225-3238, 2014.
546 Lee, D., and Hochgreb, S., Dept. of Env., Report 87AL4487, Wiley and Sons, 1998.
547 Lewis, B., and von Elbe, G., Combustion, Flames and Explosions of Gases, 3rd Ed., Chap. 2, New York
548 Acad. Press, 1987.
549 Li, J., et al., Int. J. Chem. Kinetics,, 36, 566-575, 2004.
550 Luger, R., and Barnes, R., Astrobiol., 15, 119-143, 2015.
551 Luger, R., et al., Astrobiol., 15, 57-88, 2015.
552 Maas, U., and Warnatz, J., Combustion and Flame, 74, 53-69, 1988.

553 Mills, S. M., and Abbot, D. S., ApJ, 774, 2, 2013.
554 Moses, J., et al., ApJ, 763, 25, 2013.
555 NASA factsheet Earth, http://nssdc.gsfc.nasa.gov, 2016.
556 Natarajan, J., et al., 5th US combustion meeting, March 25-27, paper A02, 2007.
557 Navarro-González, R. N., et al., J. Geophys. Res., Lett., 25, 3123-3126, 1998.
558 Ogihara, M., and Ida, S., ApJ, 699, 824-838, 2009.
559 Oliver, J. E., National Oceanic and Atmospheric Administration, Encyc. Climatology, 2005.
560 Ono, R., and Oda, T., J. Physics, Conf. Series, Electrostatics, 142, 012003, 2008.
561 Paul, P., and Warnatz, J., 27th Symposium on combustion, 495-594, 1998.
562 Pavlov, A. A., et al., J. Geophys. Res., 105, E5, 11,981-11,990, 2000.
563 Pfahl, U. J., et al., Comb. and Flame, 123, 140-158, 2000.
564 Pickering, K. E., et al., J. Geophys. Res., 103, 31,203-31,216, 1998.
565 Raymond, S., et al., ApJ, 669, 606-614, 2007.
566 Russell, C. T., et al., J. Geophys. Res., 113, E5, 10.1029/2008JE003137, 2008.
567 Schroeder, V., and Holtappels, K., Int. Conf. on Hydrogen Safety, Pisa, Italy, Sep. (8-10), 2005.
568 Schryer, D. R., Heterogeneous atmospheric chemistry, Geophysical monograph 26, 1982.
569 Schwieterman, E., et al., ApJL, 819, L13, 2016[a].
570 Schwieterman, E., et al., ApJL, 821, L34, 2016[b].
571 Segura, A., et al., Astrobiol., 5, 706-725, 2005.
572 Segura, A., et al., A&A, 472, 665-679, 2007.
573 Seinfeld, J. H., and Pandis, S. N., Atmospheric Chemistry and Physics, Wiley, 2006.
574 Seitzman, J., Georgia Tech., School of Aerospace Eng., Course Material AE/ME-6766 Combustion, 2005.
575 Selsis et al., A&A, 388, 985-1003, 2002.
576 Sichel, M., et al., Proc. Roy. Soc., 458, 49-82, 2002.
577 Sichel, M., et al., Proc . Math. Phys. Eng. Sci., 470, 2168, 2014.
578 Tian, F., et al., EPSL, 385, 22-27, 2014.
579 Tobie, G., et al., Nature, 440, 61-64, 2006.
580 Verronen, P. T., et al., J. Geophys. Res. Lett., 35, L20809, 2008.
581 Wang, X., and Law, C. K., J. Chem. Phys., 138, 134305-1, 2013.
582 Wordsworth, R. and Pierrehumbert, R., ApJL, 785, L20, 2014.
583 Yair, Y., Adv Spa. Sci. Rev., 50, 293-310, 2012.
584 Yang, J., et al., ApJL, 771, L2, 2013.

585 Yung, Y., and DeMore, W. B., Photchem,. of Plan. Atm., Oxford Uni. Press, 1999.
586 Zerkle, A. L., et al., Nature, 5, 359-363, 2012.
587 Zheng, L., et al., Int, Conf, ICEEE, 10.1109/ICEEE2010.5661000, 2010.
588 Zlochower, I.A., and Green, G. M., J. Loss. Prev. Proc. Ind., 22, 499-505, 2009.
589

590 **Appendix 1: Reaction rates (ppbv/s) related to the $H_2$-$O_2$ explosion combustion mechanism**

591 Table A1 presents key reaction rates affecting $H_2$-$O_2$ abundances at the surface for modern Earth
592 (control run, Grenfell et al., 2014) and for an Earth-like planet (values shown in brackets) orbiting in the
593 HZ of an M7 star (Grenfell et al., 2014):
594

| Reaction | Modern Earth Surface rate (ppbv/s) | Earth-like orbiting M7 Surface rate (ppbv/s) |
|---|---|---|
| $O + O + M \rightarrow O_2 + M$ | $6.5\times10^{-18}$ | $1.6\times10^{-20}$ |
| $H + H + M \rightarrow H_2 + M$ | $1.5\times10^{-25}$ | $7.1\times10^{-29}$ |
| $H + OH + M \rightarrow H_2O + M$ | $1.2\times10^{-16}$ | $1.4\times10^{-23}$ |
| $HO_2 + HO_2 \rightarrow H_2O_2 + O_2$ | $1.0\times10^{-5}$ | $6.1\times10^{-8}$ |
| $H + O_2 + M \rightarrow HO_2 + M$ | $3.3\times10^{-5}$ | $7.1\times10^{-7}$ |
| $H_2O_2 + OH \rightarrow HO_2 + H_2O$ | $2.3\times10^{-6}$ | $2.7\times10^{-12}$ |
| $H_2O_2 + hv \rightarrow OH + OH$ | $3.5\times10^{-6}$ | $1.9\times10^{-9}$ |

595

596 Table A1: Key reaction reaction rates for the $H_2$-$O_2$ explosion combustion mechanism. Data is shown for
597 surface conditions of p=1bar, T=288K for the modern Earth (control run, Grenfell et al., 2014) and for an
598 Earth-like planet with surface conditions of p=1bar, T=292K orbiting in the HZ of an M7 star (Grenfell et
599 al., 2014).
600

601 Table A1 suggests that the rates for the modern Earth case are several orders of magnitude
602 higher than the case of the Earth-like planet orbiting in the HZ of the M7 star. This is likely related to the
603 weak UV environment of the Earth-like case which leads to weak release of HOx from its reservoirs. We
604 do not anticipate that this will affect greatly the net rate of explosion-combustion however, since this
605 process is controlled by the rate of the radical-radical initiation reactions, driven by the amount of $H_2$
606 and $O_2$, lightning and cosmic rays, which are expected to be high.

607 Table A1 suggests that the production rates of the stable products $H_2$ and $O_2$ are many orders of
608 magnitude slower than those of $H_2O$ which suggests that recycling back into the reaction products $H_2$-$O_2$
609 is slow. The $H_2O_2$ budget features a balance between mainly gas-phase production from the $HO_2$
610 precursor and destruction via e.g. photolysis (and deposition).
611
612 **Appendix 2: Effect of radical removal via sticking on solid surfaces**
613 The limits of explosion/combustion are frequently determined in the laboratory using reaction
614 chambers. Sticking collisions (hence removal) of reactive of gas-phase radicals on the inner walls of the
615 chamber disfavours explosion/combustion. To estimate the role of surface chemistry for planetary
616 atmospheres, Table A2 shows the ratio surface area divided by the volume of gas (atmosphere) for a
617 range of conditions:
618

| Earth's troposphere* | Reaction chamber# | Stratospheric aerosol$ | Polluted troposphere& | Martian global dust devil## |
|---|---|---|---|---|
| $9.98 \times 10^{-5}$ | 3.00 | $1.00 \times 10^{-7}$ | $1.00 \times 10^{-4}$ | $4.83 \times 10^{-4}$ |

619 Table A2: The ratio surface area divided by the volume of gas (atmosphere) for a range of conditions.
620 *Value represents the volume shell from Earth's surface up to z=10km altitude divided by the total
621 surface area (ocean plus continents) of the Earth assuming a spherical planet. #Assuming a spherical
622 chamber with 2m diameter. $Value represents the mean stratospheric sulfate aerosol loading
623 of the modern Earth (Seinfeld and Pandis, 2006). &Schryer, 1982. ##Assuming 1000 dust particles $cm^{-3}$
624 with a radius of 1.6 microns (Esposito et al., 2011).
625 Values in Table A2 suggest that atmospheric scenarios feature lower surface/volume ratios than
626 reaction chambers used in the laboratory to determine the conditions for explosion-combustion. The
627 first and third explosion limits can be sensitive to surface reactions (Wang and Law, 2013) – in
628 atmospheres the rather low surface areas in Table A2 suggest that these limits would therefore be
629 reached more easily (at lower p, T) in planetary atmospheres compared with the laboratory-
630 determined limits. Experimental data is however lacking so further quantification of the conditions
631 where the first and third limits would be reached is the focus of future work.